



Prediction of Creep-Fatigue Interaction Damage for Polyamide 6,6 Composites

Orhan S. Abdullah* Shaker S. Hassan** Ahmed N. Al-khazraji***

*, **, *** Department of Mechanical Engineering / University of Technology

*Email: orhan_sabah@yahoo.com

**Email: Shaker_sakran1952_1@yahoo.com

***Email: dr_ahmed53@yahoo.com

(Received 26 February 2020; accepted 22 June 2020)

<https://doi.org/10.22153/kej.2020.06.001>

Abstract

This paper aims to study the damage generated due to creep-fatigue interaction behaviors in solid polyamide 6,6 and its composites that include 1%wt of carbon nanotubes or 30% wt short carbon fiber prepared by an injection technique. The investigation also includes studying the influence of applied temperatures higher than the glass transition temperatures on mechanical properties. The obtained results showed that the addition of reinforcement materials increased all the mechanical properties, while the increase in test temperature reduced all mechanical properties, especially for polyamide 6,6. The creep-fatigue interaction resistance also improved due to the addition of reinforcement materials by increasing the theoretical damage value by 50% approximately, and the failure always happened through the rotating part of the creep-fatigue interaction test program. Using the Manson-Halford damage equation to estimate the damage generated in polyamide 6,6 and its composites gives unsafe design conditions.

Keywords: *CNT_s, creep-fatigue interaction, polyamide 6,6, short carbon fiber.*

1. Introduction

Thermoplastic polymers and their composites take a considerable place in the industrial field as a result of their good chemical stability, high damage and impact resistance, low processing costs, and their good performance at elevated temperatures [1]. All these characteristics motivate to suggest thermoplastic composites to be used in automobile industry, especially in manufacturing gears, bearings, clutches, etc. all these parts will be exposed to cyclic loading and high temperatures that may be higher than their glass transition temperatures (T_g) [2, 3].

The failures of the engineering parts which are manufactured from polymers or polymer composites that operating at an elevated temperature and cyclic loading is caused by a complex phenomenon which is known as creep-

fatigue interaction, the combination of creep and fatigue effects leads to cause an accelerated failure at a time lower than that required for each creep or fatigue failure separately [4]. Creep damage, is classified as a time-temperature dependent process, which depends mainly on the values of the stress and temperature that are applied to the test specimen. In contrast, fatigue damage will occur due to cyclic loading and is basically dependent on time; therefore, it is classified as a time-dependent process. As the two kinds of damages are collected on the operating part, creep-fatigue interaction damage was inevitably developed [5].

Several authors investigated the creep-fatigue interaction behavior in metals, but a few researches are available about this interaction in polymers and their composites [4-10]. Daniel D. Samborsky et.al [6] studied the influence of the

addition of unidirectional glass fibers with 20 % wt on combined creep-fatigue behavior of biaxial woven glass fiber/epoxy composites with different test frequencies. The tests were performed at a temperature higher than T_g , and the tension-compression loading with stress ratios is equal to 0.1, -1, and 10. The results showed that the increase in test frequency reduced the time required to failure, while the addition of unidirectional glass fibers to the prepared composite improved their total time to failure. Mahir H. Majeed [7] predicted the creep-fatigue interaction damage in epoxy 135 reinforced with woven carbon fiber, according to damage energy and hysteresis loop energy values at 50°C, as well as suggesting a new method to estimate the material life by considering the relationship between damage energy and the crack area. B. Vieille et.al [8] investigated the creep-fatigue interaction behavior in laminated polyphenylene/carbon fiber composite at a temperature higher than T_g . Three different types of loads were used to create a creep-fatigue interaction effect on the test specimen. The results showed that the increase in holding time holds the test specimens at stresses higher than the threshold value causes a plastic deformation, as well as, prior the fatigue loading by creep holding results an accelerated fracture. M. Eftekhari and A. Fatemi [9] assessed the influence of temperature, frequency, load level, and holding stress on the creep-fatigue interaction and Thermal Mechanical Fatigue (TMF) behavior for different polymer composites, namely: polyamide 6,6 with 30 %wt of glass fiber, polypropylene with 30 % wt glass fiber, blend polypropylene-ether & polystyrene with 20% wt of glass fiber, and polypropylene reinforced with 40% wt of talc particles at a range of temperatures varied between 85 and 120°C. The results indicated a non-linear behavior in creep-fatigue interaction and TMF behaviors for all polymer composites, and the use of Chaboche model gives an expected life estimation. Abdolavahid Movahedi Rad et.al [10] developed a new creep-fatigue interaction model for polymer matrix composites which depends on lots of experimental fatigue data obtained from previous reviews. This new model can be used to obtain the fatigue behavior of different polymer composites when a small amount of data was available, as well as estimate the creep-fatigue interaction behavior by considering the thermal effect on fatigue behavior. Yong Guo et.al [11] assessed the low cycle fatigue-creep interaction phenomena in self-tapping screws made of high-density polyethylene

/rice husk powder composite at stress levels equal to 40, 60, and 80% of its tensile strength. The results showed that the decrease in holding time increases the fatigue damage effect and vice versa. A. Vahid Movahedi Rad et.al [12] investigated the creep-fatigue interaction behavior of laminated glass fiber epoxy composite at different stresses and holding time levels. The obtained results indicate that a short holding time has a limited interaction effect while a clear reduction in creep-fatigue interaction resistance appeared with an increase in holding time, and the failure almost happened due to fiber pull-out or matrix crazing.

In the present work, a comprehensive investigation of creep-fatigue interaction behavior for solid polyamide 6,6 reinforced with 1%wt CNT_s or 30%wt short carbon fiber will be employed at a range of stresses that varies between 70% and 90% of their yield stresses at temperatures higher than their T_g value that are equal to 50°C according to DSC test that was performed for the prepared materials.

2. Theoretical Consideration

2.1 Creep-Fatigue Interaction

The overall damage generated by combined creep and fatigue effects is completely different from separated damage generated by each loading type alone. Therefore, the influence of the creep-fatigue interaction phenomenon on thermoplastic composites is more harmful in comparison to creep and fatigue effects separately and must be considered as a design parameter; also taking into account that the duration of the holding time may create additional physical effects by the interaction of the of tested material with the environment.

To compute the damage generated due to creep-fatigue interaction effects, linear damage roles are suggested by Manson and Halford [13] that collect the damage term of creep and fatigue together and will be considered in this work as:

$$D = \sum D_f + \sum D_c = 1 \quad \dots(1)$$

where D_f and D_c are fatigue damage and creep damage respectively.

Fatigue damage can be calculated according to Miner's role for fatigue life evaluation as [14]:

$$D_f = \sum \frac{n_f}{N_{ff}} \quad \dots(2)$$

where n_f represents the experienced cycles while, N_{ff} refers to the number of cycles until failure at the selected stress and temperature.

The creep damage term can be calculated according to Robinson's equation as [15]:

$$D_c = \sum \frac{t_h}{t_r} \quad \dots(3)$$

where t_h represents the holding time in hours, while the t_r is the required time to creep rupture in hours at the selected stress and temperature. By substituting equations (2) and (3) in equation (1), the overall damage due to creep-fatigue interaction effect can be calculated according to equation (4):

$$D = \sum \frac{n_f}{N_{ff}} + \sum \frac{t_h}{t_r} \quad \dots (4)$$

As the creep-fatigue interaction program is continuously repeated until failure, two counters for each parameter must be considered. X was used as a counter for fatigue damage while Y was used for creep damage. Therefore, the experimental damage based on equation (4) will be:

$$D = \frac{n_f}{N_{ff}} \cdot X + \frac{t_h}{t_r} \cdot Y \quad \dots(5)$$

The time spent in rotating up to the failure under fatigue loading can be calculated according to equations (6) and (7) as follows:

$$t_f = \frac{n_f}{60 \times w} \quad \dots(6)$$

$$t_{ff} = \frac{N_{ff}}{60 \times w} \quad \dots(7)$$

By substituting equations (6) and (7) in equation (5), the damage equation will be:

$$D = \frac{t_f}{t_{ff}} \cdot X + \frac{t_h}{t_r} \cdot Y \quad \dots(8)$$

Thus, the theoretical total time until failure can be obtained as follows:

$$t_{cf.the} = t_f \cdot X + t_h \cdot Y \quad \dots(9)$$

In the present work, the failure always happened when the test specimens passed through the fatigue region in the creep-fatigue interaction program, therefore;

$$Y \leq X \leq Y + 1 \quad \dots(10)$$

In order to obtain a safe design, it should be assumed that the number of repeats in the fatigue region equals the number of repeats in the creep region ($X=Y$) in the creep-fatigue interaction test program. According to this assumption, the theoretical time until failure that is obtained will be lower than the actual value and gives safety in design.

By substituting $X=Y$ in equations (8) and (9), the theoretical damage value and theoretical time until failure will be calculated as follows:

$$D_{the} = Y \cdot \left[\frac{t_f}{t_{ff}} + \frac{t_h}{t_r} \right] \quad \dots(11)$$

$$t_{cf.the} = Y \cdot [t_f + t_h] \quad \dots(12)$$

The ratio of n_f/N_{ff} will be 0.2, while the ratio of t_h/t_r will be equal to 0.1. By substituting in equation (11), Y will be equal to:

$$Y = \frac{D_{the}}{0.3} \quad \dots(13)$$

And the theoretical time until failure due to creep-fatigue interaction behavior can be calculated by substituting equation (13) in equation (12) as follows:

$$t_{cf.the} = \frac{D_{the} \cdot [t_f + t_h]}{0.3} \quad \dots(14)$$

3. Experimental Details

3.1 Materials

Solid and reinforced polyamide 6,6 with 1% wt CNTs or 30% wt, short carbon fibers as reinforcement materials are received from Guangzhou Engineering Plastic Industries (Group) Co., Ltd., are tested on this work.

3.2 Composite Preparation

Solid polyamide 6,6 and its composites are prepared by an injection technique by Guangzhou Engineering Plastic Industries (Group) Co., Ltd. The materials that are used as a reinforced material are CNTs with (purity $> 95\%$, diameter: 20-25 nm, length: 25-40 μm) and short carbon fiber with (diameter: 10 μm , and average length 260 μm).

3.3. Experimental Test

3.3.1 Tensile test

A tensile test was employed at room and elevated temperatures for solid and reinforced polyamide 6,6 rod test specimens with 6 mm diameters as illustrated in figure (1) prepared according to ASTM D638 tensile test standard [16].

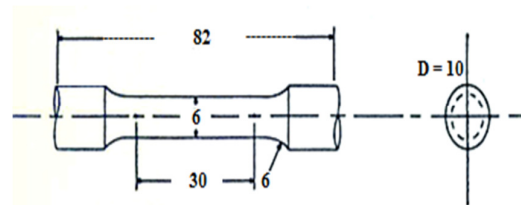


Fig. 1. Standard tensile test specimen.

3.3.2 Creep-rupture Test

In order to estimate rupture time (t_r) under creep influence, the creep-rupture test was performed at temperatures higher than T_g and applied stresses varied between 70% and 90% of yield stresses for the prepared materials according to ASTM D 2990 creep test standard as illustrated in figure (2) [17].

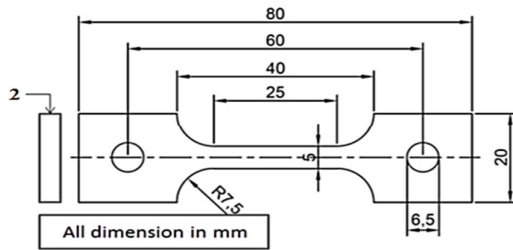


Fig. 2. Standard creep-rupture test specimen.

3.3.3 Fatigue and Creep-fatigue Interaction Tests

To predict the fatigue and creep-fatigue interaction behaviors for polyamide 6,6 and its composites at series of applied temperatures above and below their T_g , a fatigue test machine equipped with a suitable furnace was manufactured for this purpose as shown in figure (3). The test specimens for both cases were prepared according to ASTM E606 rotating bending fatigue test standard as shown in figure (4 a & b)[18].



Fig. 3. Fatigue and creep- fatigue interaction test machine.

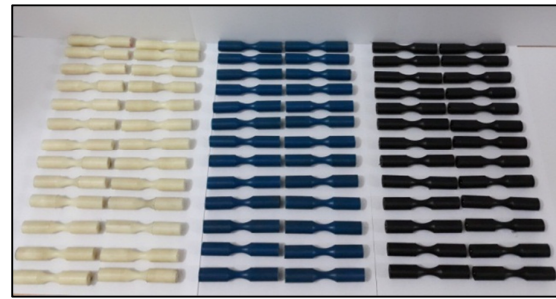


Fig. 4-a. Fatigue and creep-fatigue interaction test specimens.

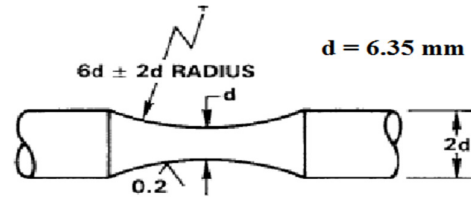


Fig. 4-b. Standard fatigue and creep-fatigue interaction test specimen.

Indeed, the creep-fatigue interaction test was based on some assumptions to generate a general equation suitable to estimate the creep-fatigue interaction behavior in polyamide 6,6 and its composites. K. Noda et.al [19] indicated that when analyzing the specimen surface of polyamide 6,6 reinforced by short glass fiber with SEM analyzer after subjected to approximately 20% of its required number of cycles to failure and testing temperature higher than the glass transition temperature that a high local stress intensity was created at the fiber ends due to microvoids generating at this zone which caused to crack initiate. On the other hand, as seen in the creep-rupture test performed in this work; the second creep stage in polyamide 6,6 and its composites were started at times nearly equal to one-tenth of its rupture time.

Based on these detections, the creep-fatigue interaction test program will be designed to rotate the test specimen for 20% of its number of cycles until failure under thermal fatigue test at the same level of applied stress and temperature, and then hold it under pure creep influence for a time equal to 10% of its time until rupture, and then the process will be repeated until the failure has happened.

4. Results and Discussion

4.4.1 Tensile Test Results

Table (1) manifests the mechanical properties for solid and reinforced polyamide 6,6 at room and elevated temperatures. It can be recognized that the addition of reinforced materials improved the mechanical properties clearly, while the increase in testing temperature leads to the reduction of these properties, especially for polyamide 6,6. The addition of CNT_s particles leads to a good improvement in σ_y , σ_u , and the modulus of elasticity values at room temperature by 53%, 52%, and 138% respectively. Within the continuous increase in testing temperature, the presence of CNT_s in polyamide 6,6 structures played an important role in preserving the mechanical properties at an accepted level, which increased the yield stress, tensile strength, and modulus of elasticity by 88%, 88%, and 100%, respectively in comparison to solid polyamide 6,6 at 130 °C.

In contrast, the addition of short carbon fibers with 30% wt raised the enhancement in σ_y , σ_u , and the modulus of elasticity values at room temperature to 116%, 112%, and 276%, respectively. This improvement in mechanical properties can be attributed to the good wettability between the fibers and the matrix, and that results a high structural polyamide 6,6 composite has the ability to serve under high tensile loading conditions. In spite of the increase in testing temperature, the improvement in mechanical properties due to the increase in short carbon fibers addition gradually increased; it increased the yield stress, tensile strength, and the modulus of elasticity by 172%, 175%, and 324% respectively in comparison to solid polyamide 6,6 at 130 °C.

Table 1,
Polyamide 6,6 and its composites mechanical properties.

Material	Temp. °C	σ_y (MPa)	σ_u (MPa)	E (GPa)
PA6,6	20	56.37	83.15	3.117
	60	39.66	57.82	2.131
	70	36.00	52.54	1.926
	80	32.32	46.88	1.7
PA6,6+ 1%CNT _s	20	86.62	126.41	7.42
	60	63.40	92.25	5.47
	70	57.33	83.73	4.9
PA6,6+ 30%CF	80	53.00	77.41	4.4
	20	121.9	176.38	11.73
	60	94.53	136.27	8.8
PA6,6+ 30%CF	70	88.23	127.18	8.1
	80	81.30	117.21	7.38

4.4.2 Creep-rupture Test Results

One of the most important parameters obtained from the creep-rupture test was the time to rupture (t_r), due to its importance in the estimation of creep-fatigue interaction damage values. Table (2) listed the time to rupture of all tested materials, and it can be seen that reinforced polyamides 6,6 have a longer time to rupture than solid polyamide 6,6, as well as that the increase in applied stress and temperature decreases the time to rupture values for all cases. This behavior was attributed to the fact that any increase in applied temperature higher than the T_g will increase the mobility of molecular chains, and finally results in a high deformation level, while with the presence of reinforcement materials, the molecular chains were restricted and the composite showed a high resistance against deformation. High compatibility in creep behavior of PA6,6 composites were obtained in this work with creep behavior indicated by Yu Jia et al. [20] and Yi Luen Li et al. [21] due to the addition of MWCNT_s to the polypropylene and epoxy resins, respectively.

Table 2,
The time to rupture values for solid and reinforced polyamide 6,6.

Material	σ/σ_y	Time to rupture t_r (hr.)		
		60°C	70°C	80°C
PA6,6	0.70	62.13	57.35	48.12
	0.75	48.42	44.32	39.76
	0.80	38.53	35.37	31.48
	0.85	30.61	28.22	25.23
	0.90	26.54	22.54	18.89
PA6,6+ 1%CNT _s	0.70	86.43	77.34	63.66
	0.75	71.52	62.72	50.32
	0.80	53.92	47.31	37.44
	0.85	43.31	36.16	30.11
	0.90	33.22	28.71	22.18
PA6,6+ 30%CF	0.70	97.43	86.28	77.12
	0.75	80.32	71.42	61.33
	0.80	65.35	56.43	46.26
	0.85	53.66	44.82	34.87
	0.90	41.57	33.78	26.24

4.4.3 Fatigue Test Results

Pure fatigue and isothermal fatigue tests are employed with fully reversed loading (R=-1) for the prepared materials in order to achieve the number of cycles until its failure at each applied stress and temperature level. It is shown in figures (5, 6, and 7) that the increase in applied stress and temperature reduces fatigue life while the addition of CNT_s and short carbon fibers enhances fatigue

life broadly. The reinforcement materials played an important role in the inherent fatigue resistance in polyamide 6,6, by preventing the microcracks that initiated owing to cyclic loading from propagation as possible, the initiated microcracks were united with each other to create one main crack, which causes the failure. In solid polyamide 6,6, a number of microcracks were initiated and propagated without a deterrent in the loading direction, which caused a crazing failure mechanism. In contrast, with environmental temperature increases, the probability of chain scission increases too, due to the internal heat generation, and the weak heat dissipation to the surrounding polymers leads to accelerate the fatigue failure. With the presence of reinforcement materials, the molecular chains were restricted, and their mobility was limited and the failure required a long time to happen.

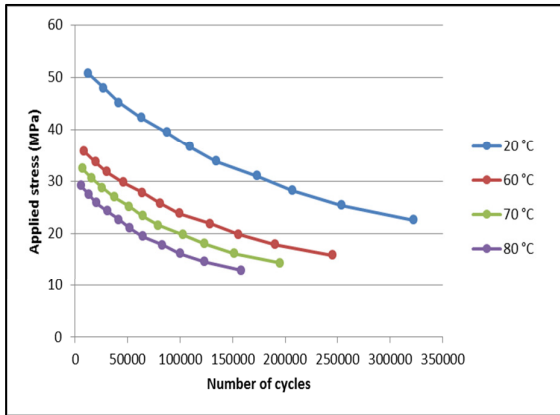


Fig. 5. The S-N curves for polyamide 6,6 at several temperatures.

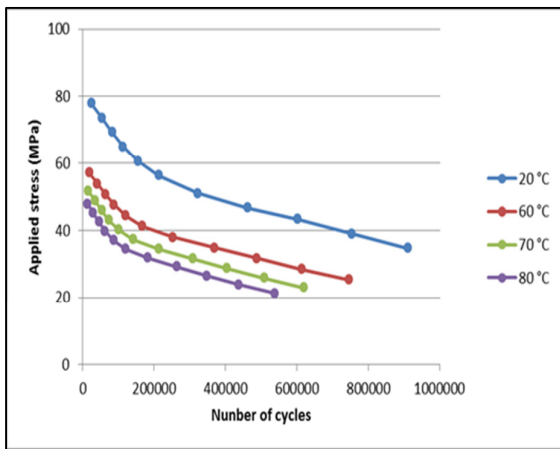


Fig. 6. The S-N curves for polyamide 6,6 + 1% CNTs at several temperatures.

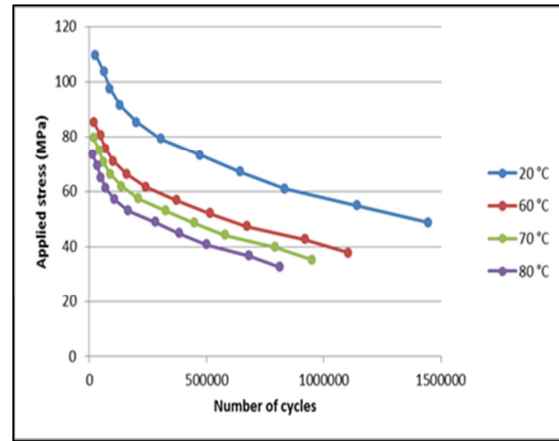


Fig. 7. The S-N curves for polyamide 6,6 + 30% CF at several temperatures.

4.4.4 Creep-Fatigue Interaction Results

Tables (3, 4, and 5) reported the creep-fatigue interaction damage for polyamide 6,6 and its composites. It can be noticed that the values of X and Y are equal to two for polyamide 6,6 while it equals to three for PA66/CNT and PA66/CF composites, this variation in X and Y values can explain the influence of reinforcement materials on creep-fatigue interaction resistance. The test program was always started by fatigue cycling which caused a crack initiation due to rotating the test specimen for n_f cycles and then followed by a period of holding time at certain temperatures caused a crack propagation as illustrated in figure (8), for polyamide 6,6, the second block in test program accelerated the crack propagation, and within the start of the rotating part in block three, the failure has happened.

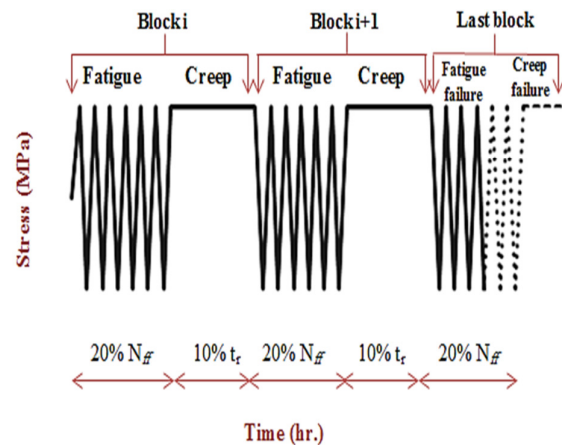


Fig. 8. The creep-fatigue interaction test program

The failure mechanism in polyamide 6,6 can be summarized as a chain scission that occurs due to localized heat at a crack tip generated by cyclic loading leads to accelerate crack propagation and failure. On the other hand, polyamide 6,6 composites, after rotating and holding the test specimen for a period of time as considered in first block of test program, microvoids were generated in the interface region between the matrix and reinforcement materials. In spite of continuity in applied cyclic loading and holding the test specimen for a period of time under creep influence for two additional block programs, the failure has not happened. This can be explained that the reinforcement materials prevent the accelerated failure by preventing microcracks that initiated near the fiber sides or grain boundaries of nano particles from propagation as possible, but the nucleation of new microcracks was continuous.

With an increase in microcracks in the interface region, a debonding phenomenon occurs

along the fiber side or nano grain boundaries leads to create cracked walls by connecting the microcracks together, which weakens the composite material, and then finally fractures it with ductile manner under cyclic loading in the fourth block of creep-fatigue interaction program. Furthermore, from obtained results, it can be observed that the increase in stress amplitude and temperature accelerated the failure by reducing the time required until its fracture.

It can be seen that the experimental damage values for all cases are less than one; these results are not compatible to the Manson Halford rule which assumed the total damage for creep-fatigue interaction should be equal to one, as well as the total number of cycles until the failure under creep-fatigue interaction behavior is lower than the required numbers of cycles until failure under only fatigue effect and the total time until failure due to interaction was also lower than the rupture time due to only creep influence.

Table 3,
Summary of creep-fatigue interaction damage for polyamide 6,6.

Temp. °C	σ/σ_y	n_r (cycle)	N_{fr} (cycle)	X	D_r	t_h	t_r	Y	D_C	D_{total}
60	0.70	12766	63830	2.12	0.424	6.213	62.13	2	0.2	0.624
	0.75	9112	45560	2.14	0.428	4.842	48.42	2	0.2	0.628
	0.80	5965	29825	2.08	0.416	3.852	38.52	2	0.2	0.616
	0.85	3844	19220	2.11	0.422	3.061	30.61	2	0.2	0.622
	0.90	1689	8445	2.09	0.418	2.654	26.54	2	0.2	0.618
70	0.70	10238	51190	2.14	0.428	5.735	57.35	2	0.2	0.628
	0.75	7450	37250	2.02	0.404	4.432	44.32	2	0.2	0.604
	0.80	5102	25510	2.18	0.436	3.537	35.37	2	0.2	0.636
	0.85	3157	15785	2.02	0.422	2.822	28.22	2	0.2	0.622
	0.90	1390	6950	2.07	0.414	2.254	22.54	2	0.2	0.614
80	0.70	8258	41290	2.08	0.416	4.812	48.12	2	0.2	0.616
	0.75	6079	30395	2.14	0.428	3.976	39.76	2	0.2	0.628
	0.80	3988	19940	2.09	0.418	3.148	31.48	2	0.2	0.618
	0.85	2572	12860	2.11	0.422	2.523	25.23	2	0.2	0.622
	0.90	1126	5630	2.03	0.406	1.889	18.89	2	0.2	0.606

*Where X: The total rotating cycles/ n_r , and Y: The total holding time/ t_h .

Table 4,
Summary of creep-fatigue interaction damage for polyamide 6,6 + 1% CNTS.

Temp. °C	σ/σ_y	n_f (cycle)	N_{fr} (cycle)	X	D_f	t_h	t_r	Y	D_C	D_{total}
60	0.70	23990	119950	3.04	0.608	8.643	86.43	3	0.3	0.908
	0.75	17413	87065	3.16	0.632	7.152	71.52	3	0.3	0.932
	0.80	12608	63040	3.12	0.624	5.392	53.92	3	0.3	0.924
	0.85	8132	40660	3.11	0.622	4.331	43.31	3	0.3	0.922
	0.90	3625	18125	3.34	0.668	3.322	33.22	3	0.3	0.968
70	0.70	20208	101040	3.17	0.633	7.734	77.34	3	0.3	0.933
	0.75	14604	73020	3.21	0.642	6.272	62.72	3	0.3	0.942
	0.80	11518	35035	3.11	0.675	4.731	47.31	3	0.3	0.975
	0.85	6866	34330	3.09	0.618	3.616	36.16	3	0.3	0.918
	0.90	3053	15265	3.11	0.621	2.871	28.71	3	0.3	0.921
80	0.70	17174	85870	3.12	0.621	6.366	63.66	3	0.3	0.921
	0.75	12402	62010	3.19	0.638	5.032	50.32	3	0.3	0.938
	0.80	9007	45035	3.14	0.628	3.744	37.44	3	0.3	0.928
	0.85	5770	28850	3.09	0.618	3.011	30.11	3	0.3	0.918
	0.90	2576	12880	3.11	0.622	2.218	22.18	3	0.3	0.922

*Where X: The total rotating cycles/ n_f , and Y: The total holding time/ t_h .

Table 5.
Summary of creep-fatigue interaction damage for polyamide 6,6 + 30% CF.

Temp. °C	σ/σ_y	n_f (cycle)	N_{fr} (cycle)	X	D_f	t_h	t_r	Y	D_C	D_{total}
60	0.70	31684	158420	3.42	0.684	9.743	97.43	3	0.3	0.984
	0.75	20422	102110	3.38	0.676	8.032	80.32	3	0.3	0.976
	0.80	13475	67375	3.41	0.682	6.535	65.35	3	0.3	0.982
	0.85	9525	47630	3.34	0.668	5.366	53.66	3	0.3	0.968
	0.90	4070	20350	3.43	0.686	4.157	41.57	3	0.3	0.986
70	0.70	27440	137200	3.47	0.694	8.628	86.28	3	0.3	0.994
	0.75	17768	88440	3.45	0.693	7.142	71.42	3	0.3	0.993
	0.80	11892	59460	3.38	0.676	5.643	56.43	3	0.3	0.976
	0.85	8373	41865	3.40	0.680	4.482	44.82	3	0.3	0.980
	0.90	3568	17840	3.43	0.686	3.378	33.78	3	0.3	0.986
80	0.70	21498	107490	3.45	0.690	7.712	77.12	3	0.3	0.990
	0.75	13786	68930	3.44	0.688	6.133	61.33	3	0.3	0.988
	0.80	9814	49070	3.38	0.676	4.626	46.26	3	0.3	0.976
	0.85	6648	33240	3.41	0.682	3.487	34.87	3	0.3	0.982
	0.90	2884	14420	3.39	0.678	2.624	26.24	3	0.3	0.978

*Where X: The total rotating cycles/ n_f , and Y: The total holding time/ t_h .

In fact, the theoretical damage values that were obtained according to equation (11) have a high compatibility with experimental damage values that are listed in tables (3, 4, and 5), and in order to obtain a safety design under creep-fatigue interaction behavior for polyamide 6,6 and its composites, the values of D_{the} should be lower

than the experimental values and should be limited within the following ranges:

For polyamide 6,6:

$$0 \leq D \leq 0.6$$

For reinforced polyamide 6,6:

$$0 \leq D \leq 0.9$$

The experimental results of the damage value vary between 0.604 and 0.636 with an average value equal to 0.62 for solid polyamide 6,6, while it varied between (0.904 -0.975) and (0.968-0.994) with average values of 0.931 and 0.98 for polyamide 6,6 +1% CNT_s and polyamide 6,6 +30% CF respectively. All experimental damage values are higher than the theoretical damage values, and this indicates that the initial assumption that is considered for creep-fatigue interaction behavior gives a safety design.

Finally, according to the obtained theoretical damage values D_{the} , a general amplitude interaction diagram can be plotted for polyamide 6,6 and its composites which is suitable for safety design under the influence of creep-fatigue interaction within a range of temperatures that varies between room temperature and 80 °C since there was no variation in experimental damage values that was seen with temperature change.

Figures (9 and 10) illustrated the general amplitude interaction diagrams for polyamide 6,6 and its composites. It can be seen clearly that the addition of carbon fibers or carbon nanotubes increases the safe design zone under the influence of creep-fatigue interaction conditions by 50%. A high agreement in general amplitude interaction diagrams was achieved in this work that was obtained by J. Bowman and B. Barker [22] when investigated the methodology for describing the creep-fatigue interaction damage in polymers and their similarity to metal.

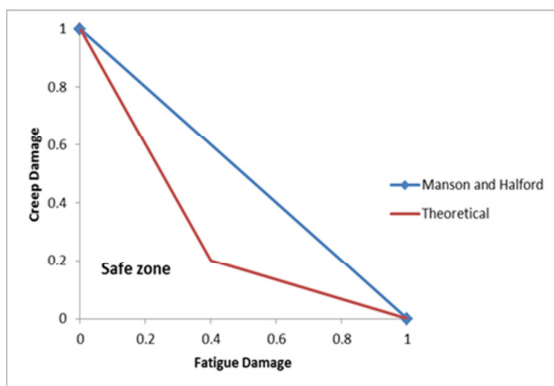


Fig. 9. The general amplitude interaction diagrams for polyamide 6,6.

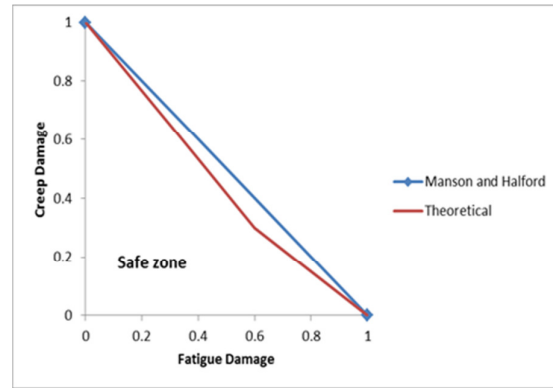


Fig. 10. The general amplitude interaction diagrams for both polyamide 6,6 composites.

5. Conclusions

According to the results above, the following can be concluded:

1. The addition of CNT_s and short carbon fibers to polyamide 6,6 improved their tensile strength, modulus of elasticity, yield stress, creep rupture time, and fatigue life.
2. The increase in test temperature reduced all the mechanical properties and accelerated the failure.
3. In all creep-fatigue interaction test specimens, the failure always happened during the rotating part in the test program.
4. The consideration of the Manson-Halford assumption to predict the damage generated due to creep-fatigue interaction behavior gives unsafe designs for polyamide 6,6 and its prepared composites.
5. The addition of reinforcement materials increased the creep-fatigue interaction resistance by increasing the theoretical damage value by 50% in comparison to the value of polyamide 6,6.

6. References

- [1] Orhan S. Abdullah, 'Experimental study to the effect of natural particles added to unsaturated polyester resin of a polymer matrix composite', Al-Khwarizmi engineering journal, Vol.13, No. 1, P.P. 42-49, 2017.
- [2] S. Rajesh Kumar, Dr.Mannan and V. Bakkiyaraj, 'Development of thermo plastic gears for heavy duty applications using APDL', International journal of trend research and development, vol. 3, no. 2, pp. 304-309, 2016.

- [3] Ibtihal A. Mahmood, Wafa A. Soud, Orhan S. Abdullah, 'Effects of different types of fillers on dry wear characteristics of carbon-epoxy composite', *Al-Khwarizmi engineering journal*, Vol.9, No. 2, P.P. 85-93, 2013.
- [4] M. Eftekhari and A. Fatemi, 'Tensile, creep and fatigue behaviours of short fibre reinforced polymer composites at elevated temperatures: A literature survey', *Fatigue Fract. Eng. Mater. Struct.*, vol. 38, no. 12, pp. 1395–1418, 2015
- [5] S. Mortazavian and A. Fatemi, 'Fatigue behavior and modeling of short fiber reinforced polymer composites including anisotropy and temperature effects', *Int. J. Fatigue*, vol. 77, pp. 12–27, 2015.
- [6] Daniel D. Samborsky, John F. Mandell, and David A. Miller, 'Creep/fatigue behavior of resin infused biaxial glass fabric laminate', *Alaa SDM Wind energy session*, 2013.
- [7] Mahir H. Majeed, 'Prediction of damage energy under creep-fatigue interaction in polymer matrix composite', *Journal of Kerbala University*, vol. 11, no.3, pp. 119–126, 2013.
- [8] B. Vieille, W. Albouy, and L. Taleb, 'about the creep-fatigue interaction on the fatigue behaviour of off-axis woven-ply thermoplastic laminates at temperatures higher than T_g', *Composites Part B*, vol. 58, pp. 478–486, 2014.
- [9] M. Eftekhari and A. Fatemi, 'Creep-fatigue interaction and thermo-mechanical fatigue behaviors of thermoplastics and their composites', *Int. J. Fatigue*, vol. 91, pp. 136–148, 2016.
- [10] A. Movahedi-Rad, T. Keller, and A. P. Vassilopoulos, 'Creep-fatigue interaction in composite materials', *ECCM 2016 - Proceeding 17th Eur. Conf. Compos. Mater.*, no. June, pp. 26–30, 2016.
- [11] Y. Guo, D. Li, S. Zhu, and Y. Chen, 'Interaction of low cycle fatigue and creep in biomass-filled plastic composites', *BioResources*, vol. 13, no. 2, pp. 3250–3258, 2018.
- [12] A. V. Movahedi-Rad, T. Keller, and A. P. Vassilopoulos, 'Creep effects on tension-tension fatigue behavior of angle-ply GFRP composite laminates', *Int. J. Fatigue*, vol. 123, pp. 144–156, 2019.
- [13] S. S. Manson and Gray Halford, 'A method of estimation high temperature low cycle fatigue behavior of materials, In: *Thermal and High Strain Fatigue*', Monograph and Report Series No. 32, Institute of Metals, London, pp. 154 – 170,
- [14] Miner, M.A. 'Cumulative damage in fatigue', *Journal of Applied Mechanics*, Vol.12, pp.159–164, 1945.
- [15] Robinson, E.L, 'Effect of temperature variation on the long-time rupture strength of steel', *Trans. ASME*, Vol. 74, pp. 777–781, 1952.
- [16] ASTM D 638 'Standard Test Method for tensile properties of plastics', *ASTM International*, West Conshohocken, PA; 2009.
- [17] ASTM D 2990 'Standard Test Methods for Tensile, Compressive, and Flexural Creep and Creep-Rupture of Plastics', *ASTM International*, West Conshohocken, PA; 2009.
- [18] ASTM E-606 'Standard recommended practice for constant-amplitude fatigue test', *ASTM International*, West Conshohocken, PA; 2006.
- [19] K. Noda, A. Takahara, and T. Kajiyama, 'Fatigue failure mechanisms of short glass-fiber reinforced nylon 66 based on nonlinear dynamic viscoelastic measurement', *Polymer*, Vol. 42, No. 13, pp.5803-5811, 2001.
- [20] Y. L. Li, M. Y. Shen, W. J. Chen, C. L. Chiang, and M. C. Yip, 'Tensile creep study and mechanical properties of carbon fiber nano-composites', *J. Polym. Res.*, vol. 19, no. 7, 2012.
- [21] Z. Yao, D. Wu, C. Chen, and M. Zhang, 'Creep behavior of polyurethane nanocomposites with carbon nanotubes', *Compos. Part A Appl. Sci. Manuf.*, vol. 50, pp. 65–72, 2013.
- [22] J. Bowman and B. Barker, 'A methodology for describing creep-fatigue interactions in thermoplastic components', *Polymer engineering and science*, Vol. 26, No. 22, pp.1582-1590, 1986.

التنبؤ بالضرر الناتج من تداخل الزحف مع الكلال لمتراكبات البولي أميد ٦,٦

أورهان صباح عبدالله* شاكرا سكران حسن** أحمد نايف الخزرجي***

،،*** قسم الهندسة الميكانيكية/الجامعة التكنولوجية

*البريد الإلكتروني: orhan_sabah@yahoo.com

**البريد الإلكتروني: Shaker_sakran1952_1@yahoo.com

***البريد الإلكتروني: dr_ahmed53@yahoo.com

الخلاصة

يهدف هذا البحث إلى دراسة الضرر الناتج من تداخل سلوك الزحف مع الكلال لمادة البولي أميد ٦,٦ ومتراكباتها التي تحتوي على انابيب الكربون النانوية بكسر وزني مقداره ١% أو الياف الكربون القصيرة بكسر وزني ٣٠% المحضرة بطريقة القولبة بالحقن. الدراسة تضمن أيضاً التحقق من الخواص الميكانيكية للمواد المحضرة عند درجات حرارية أعلى من درجة حرارة تحولها الزجاجي. أظهرت النتائج المستحصلة أن إضافة مواد التدعيم قد حسنت من قيم الخواص الميكانيكية ولكن الزيادة في درجات الحرارة المطلقة أدت إلى خفض جميع الخواص الميكانيكية وخصوصاً لمادة البولي أميد ٦,٦ الغير مدعمة. وكذلك أن إضافة مواد التدعيم قد حسنت من مقاومة تداخل الزحف مع الكلال بزيادة قيمة الضرر النظري بمقدار ٥٠% تقريباً، وأن حالة الفشل حدثت دائماً خلال الجزء الخاص بالكلال من نظام اختبار تداخل الزحف مع الكلال وأن اعتماد قانون Manson-Halford لتخمين الضرر لمادة البولي أميد ٦,٦ ومتراكباتها يعطي نتائج غير آمنة لأغراض التصميم.